IIT Ropar
List of Recent Publications with Abstract
Coverage: October, 2023

Sl. No.	
1.	3D porous sulfur-graphdiyne with splendid electrocatalytic and energy storage application I Muhammad, S Ahmed, H Cao…R Ahuja… - Materials Today Chemistry, 2023 **Abstract** The blooming emergence of graphdiyne featuring embellished sp-hybridized carbons has been highly alluring for electrocatalysis and ion storage. Here, a porous 3D material sulfur-graphdiyne (3D-SGDY) is theoretically designed comprising butadiyne chains and sulfur as a heteroatom, owing a stable cubic skeleton and an atypical tuneable indirect bandgap. Compared to sp^2-bonded carbon materials, the existence of sp-bonded carbon in 3D-SGDY tuned the direction of organic reactions leading to a single carbon product with numerous storage sites for the metal ions. Anchoring a single Cu atom in 3D-SGDY, we realize the unique Cu–C (3D-SGDY) chemical bonds exhibiting unconventional selectivity for CO_2 reduction. The Cu–C bond in 3D-SGDY predominantly forms the *OCHO intermediates in lieu of *COOH and provides an active charge deportation channel during the reduction process of CO_2 into CH_4 product. Additionally, the porous structure reveals its astounding potential as an anode material by facilitating rapid transportation with a very low diffusion barrier of 0.06 eV and an ultrahigh capacity of 1826.4 $mAhg^{-1}$ for Ca-ions. This work not only provides the 3D prototype of GDY but also administers the atomic level selectivity for CO_2RR and high-performance Ca-ion batteries.
2.	A case for amplifying row hammer attacks via cell-coupling in DARM devices K Goswami, S Das, S Satapathy, DS Banerjee - Proceedings of the 2022 International Symposium on Memory Systems, 2022 **Abstract** Main memory technologies have been largely dominated by Dynamic Random Access Memory (DRAM) for several decades. However, the recurring issue of higher latency has compelled researchers to propose In-DRAM based caching techniques. In-DRAM caches have become a popular research topic in recent years as they offer significant improvements over conventional DRAM devices. With every generation, DRAM devices are engineered to be denser. This has caused the emergence of electromagnetic interference within the device, known as row hammering, which causes flipping of bits without accessing the bits. Our work demonstrates the existence of a new and amplified row hammer attack, which, we term as double row hammer attack. It poses a simultaneous threat to both the DRAM array and the In-DRAM cache. We then propose an In-DRAM caching technique, called CRATAR, which can detect the aforementioned malicious memory pattern. Mitigating row hammer attacks impose some blocking time on the DRAM device. CRATAR is designed in a way that it mitigates double row hammer attacks in the most optimal time possible. Overall, we gain an average performance improvement of 6.74% over a conventional DDR4 DRAM. It reduces 24.71% blocking time previously imposed during mitigating row hammer attacks at the meager storage overhead of 3.88 KB.
3.	A comparative study of computational modelling frameworks for structural assessment of reinforced concrete beam O Mishra, P Haldar, ANR Chowdhury, Proceedings of 17th Symposium on Earthquake Engineering (Vol. 2): Book Chapter, 2023 **Abstract** Computational models play an important role in assessing the structural response of reinforced concrete (RC) buildings under seismic excitation. The computational modelling frameworks available for RC structures are (i) macro-element modelling, (ii) high fidelity 3D finite element modelling and (iii) multi-scale modelling with the adoption of sub-structure technique. Macro-

	element models are computationally least demanding but require extensive calibration for simulating the inelastic responses of RC members and connections with complex details. Further, 3D finite element models require minimal calibration for modelling complex RC members and connections but are computationally challenging. In contrast, the multi-scale computational framework adopts 3D finite element modelling at complex detail regions and macro-elements for the rest of the structure to provide a balance between computational efficiency and calibration complexity. This paper presents the simulation of an RC beam under linear and nonlinear analysis along with the analytical or experimental validation to access the efficacy of abovementioned computational frameworks for modelling the elastic and inelastic responses of RC structures. Considering experimental results as the benchmark while predicting the inelastic response; capacity curve, estimated toughness and the computation time were used to compare the reliability and computational efficiency of abovementioned modelling frameworks. The findings show that all three computational frameworks can predict the elastic response of an RC beam close to analytical results. However, the 3D finite element and multi-scale models gave better prediction of the inelastic response of the RC beam in comparison with macro-element model. The computation time taken by the three modelling techniques was maximum for the 3D finite element, intermediate for the multi-scale and minimum for the macro-element model. Hence, obtained results validate the computational efficacy of multi-scale model while predicting the inelastic response of a structure accurately.
4.	A comprehensive decision support system for the characterization of probability distribution tails for daily precipitation N Gupta, SR Chavan - Journal of Hydrology, 2023 **Abstract** A conventional Decision Support System (DSS) can be used to characterize tails of probability distributions into distribution families using various graphical methods. Existing DSSs lack efficient segregation of the Lognormal distribution from the Regularly varying and Subexponential distribution families. Also, they lack the ability to identify the distributions from the hyper-exponential distributions. Recently developed graphical diagnostic tools, such as concentration profile, concentration adjusted expected shortfall, discriminant moment ratio plot, maximum-to-sum plot, and Zenga plot can classify the tails of distributions into various classes if used in an appropriate order in combination with tools of conventional DSS. The present study proposes a comprehensive DSS that alleviates the shortcomings associated with the conventional DSS and characterizes the tails of distributions into classes B\A (Pareto type), C\B (regularly varying), D\C (subexponential), E (Exponential type), hyper-exponential class (outside class E) and LN (Lognormal) distribution (the limiting case between class C and D). The robustness of the proposed DSS over the conventional DSS is established through a simulation experiment. Further, this study also evaluates the influence of the sample size on the effective implementation of the proposed DSS. Finally, the proposed DSS is applied to characterize the tails of daily gridded precipitation data over India. Results indicate that precipitation data from about 98% of grids over India exhibit distributions from heavy-tailed families. The study recommends the use of heavy-tailed distributions to model daily precipitation data over India. The study also suggests that one should rely on more than one graphical method for deducing rational conclusions regarding tail characterization.
5.	A data-driven ANN model for estimation of melt-pool characteristics in SLM process R Kumar, D Bombe, A Agrawal - Manufacturing Letters, 2023 **Abstract** The Selective Laser Melting (SLM) process is layered to manufacture a near-net-shaped metallic 3D component. The SLM process involves multiple physical phenomena during part fabrication. A highly intense moving laser heat source causes rapid temperature rise leading to melting and flow of raw material in the melt-pool and subsequent solidification during the process. The

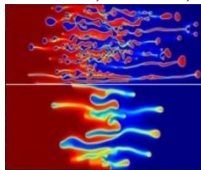|	
	present study develops an analytical model by considering various physical phenomena of the SLM process, such as heat transfer, fluid flow, the Marangoni effect, etc. It is solved using an in-house developed analytical formulation based upon Finite Volume Method (FVM) approach. Further, a data-driven machine-learning based on an Artificial Neural network (ANN) model with feedforward neural architecture was trained to estimate the melt-pool dimensions for the single-track SLM process. The developed ANN model was tested for Ti6Al4V alloy by considering all the thermo-physical material properties. A total of 1224 datasets were generated using the analytical formulation to train, validate, and test the neural network. The 70–80% of the training, validation, and testing data fall between the deviation range of 23.55 μm and −21.96 μm. The model predicts melt-pool characteristics with an average error of 0.085%, 0.053%, and 0.056% for depth, width, and length, respectively.
6.	A dynamic hard domain-induced self-healable waterborne poly(urethane/acrylic) hybrid dispersion for 3D printable biomedical scaffolds S Morang, JH Rajput, … A Poundarik, B Das… - Materials Advances, 2023 **Abstract** Polyurethane (PU) with its efficient self-healing ability and high mechanical properties is highly anticipated but an arduous challenge to achieve. In this study, to create a win-win situation, a new strategy was introduced which is based on the triple synergistic effect of a 'dynamic hard domain', 'multiple hierarchical hydrogen bonding', and 'semi-interpenetrating network (IPN) formation'. The dynamic disulfide bond of 2-APDS and multiple hierarchical hydrogen bonding raised from urea and urethane linkages supplement the healing ability, and concurrently, the polyacrylates and rigid aromatic moiety improve the mechanical properties of the SWPUA films. Owing to the judicious molecular engineering and aforementioned tactic, a series of self-healable waterborne PU/polyacrylic (SWPUA) films were prepared by using bis(2-aminophenyl) disulfide (2-APDS) as the 'dynamic hard domain', monoglyceride of castor oil (MG_{CO}) as a chain extender, glycerol ester of citric acid (GECA) as an internal emulsifier and different acrylate monomers with other desired reactants (polyols/diamines and diisocyanate). The resulting films exhibit good mechanical robustness, high thermal stability, and biodegradability. Notably, a maximum healing efficiency of 82.53% can be achieved within 330 s under microwave exposure (800 W) and the cut films were re-processable at 60 °C under a pressure of 60-80 kg cm^{-2}. Most importantly, the MTT and live/dead assays of mouse fibroblast cell lines (L929) treated with the SWPUA-2 dispersion (up to 30%) confirmed its biocompatibility. Most interestingly, SWPUA-2 can be employed to prepare a SWPUA-2/methacrylate anhydride-modified gelatin (GelMA)/gelatin hybrid ink for the development of 3D printable biomedical scaffolds.
7.	A self-calibration logic circuit agnostic to offset calibration technique for high-precision dynamic comparator N Sharma, RK Srivastava, V Hande, D Sehgal, DM Das - IEEE Women in Technology Conference (WINTECHCON), 2023 **Abstract** This paper proposes a calibration technique agnostic calibration logic circuitry for the self-calibration of the high-precision dynamic comparator, which can be used in major self-calibration techniques to activate the calibration and offset polarity change detection for completion of the calibration. This paper also briefly reviews the different comparator offset cancellation techniques, i.e., auto-zeroing, self-calibration, and chopper stabilization. The proposed calibration logic is implemented in a dynamic comparator's effective trans-conductance controlled offset calibration in SCL 180 nm technology. The standard deviation of the input-referred offset of the comparator is reduced to 445 μV from 2.85 mV with a complete calibration range of 5σ offset, therefore qualifying it for high-speed flash ADCs and asynchronous SAR ADCs. The power consumption at 1 GHz operating frequency is 154.6 μW.

8.	[A Two Stage Miller OpAmp with Low Voltage Cascode Current Source with High EMI Immunity](#) Shivdeep, S Sharma… DM Das - International Symposium on Electromagnetic Compatibility - EMC Europe, 2023 **Abstract** Electromagnetic Interference (EMI) at the input of an Operational Transconductance Amplifier (OTA) leads to a DC offset voltage at the output. The amount of EMI-induced offset depends on the frequency and amplitude of the interferer signal. Various phenomena are dominant at different frequencies, such as the asymmetric slew rate is responsible for offset induced at frequencies around the Unity Gain Frequency (UGF). This paper identifies the causes and presents a design approach to optimize the slew rate and reduce the output offset without using overhead area and power. Channel length modulation of the tail current source transistor and its reduced impedance is due to the effective capacitance (C_T) at the tail node becoming the culprit and adding more asymmetry to the slew rate. This is addressed using the cascode tail current source and additional gate-to-source capacitance C_{gsx}. Two-stage Miller OTA is designed in the standard 0.18 μm CMOS technology. Monte Carlo and the post-layout simulation results are presented to consider the parasitics, process variations, and mismatch effects.
9.	[Ab initio study of Li-shrouded Si-doped ϒ-Graphyne nanosheet as propitious anode in Li-ion batteries](#) N Duhan, TJ Dhillip Kumar – Applied Surface Science, 2024 **Abstract** Li-ion batteries (LIBs) have become a house-hold name in the energy-storage research community in the wake of their noteworthy attributes. With increasing energy demands, the urgency to develop high performance LIBs is also rising rapidly which has compelled the researchers to design and fabricate new high capacity materials. Bearing that in mind, we have investigated a carbon–silicon based anode, i.e. Si-doped ϒ -Graphyne (SiG) nanolayer for its applicability as LIB electrode. Carbon and Silicon are two complementary choices for anode material due to the reason that the weakness of one is complemented by the other i.e. the extensive volume changes of Si anodes is compensated by the stable carbon matrix and the lower Li affinity of carbon is complemented by large capacities of Si anode. The Density Functional Theory (DFT) based studies reveal that SiG nanolayer has a dynamically and thermally stable structure with reliable mechanical properties. Density of states (DOS) calculation substantiates the good conductivity of the nanolayer. The binding energy of the Li atom (adatom) is −1.33 eV resulting from a charge transfer of 0.88e from Li to the nanolayer. The SiG anode achieved a specific capacity of 1005.05 mAhg^{-1} (almost 2.7 times the Graphite anode used in commercial LIBs). Climbing Image-Nudged Elastic Band (CI-NEB) calculations depict an easy migration of the adatoms through the anode with an energy barrier of 0.67 eV having diffusion coefficient (D) as 8.91×10^{-14} cm2/s. A low working voltage of 0.44 V is obtained advocating a safe operation and good cyclability. So, the theoretical investigation presents favorable outcomes for Si-doped ϒ-Graphyne to be applicable as a progressive anode in next-generation LIBs.
10.	[Advancement of machine learning and image processing in material science](#) A Pratap, N Sardana - Industry 4.0: Concepts, Processes and Systems: Book Chapter, 2023 **Abstract**

	Machine Learning (ML) has evolved as the most widely used artificial intelligence (AI) technique for several individuals, institutions, and companies who want to automate their business. This is because the computational power has been increased and data accessibility has become easy. This allows various researchers to get a meaningful interpretation from the available data. Artificial intelligence (AI) has deeply impacted the production system and led us to a new era of the industrial revolution known as Industry 4.0. Material is a basic building block of any production system. This has created a quest between material scientists for material discovery and development. In this work, various image processing modules, libraries, and frameworks have been listed along with the problem and solution associated with them. Subsequently, the different data ecosystems which can be useful for data collection and preparation before selecting any ML model are highlighted. Furthermore, the various opportunities and challenges that material scientists have been facing in the development of new materials are also outlined for a better understanding of ML-based image processing in material science and engineering. In the end, SWOT analysis has been done using ML in material science and engineering.
11.	[Analyzing the impact of parasitics on a CMOS-Memristive crossbar neural network based on winner-take-all and Hebbian rule](#) SA Thomas, R Sharma, DM Das - Memories: Materials, Devices, Circuits and Systems, 2023 **Abstract** For cognitive tasks and classifications, neuromorphic systems have shown great potential. This paper presents a novel architecture using CMOS memristive synapses where the memristors are trained using the Hebbian rule, and the winner-take-all mechanism is used for the recognition task. The proposed architecture offers a simplified approach compared to previous state-of-the-art works, making it accessible for implementing pattern recognition tasks with in-memory computation. As the size of the memristive switching devices is in the nanometer scale, designing, modeling, and optimizing the system becomes increasingly complex. This complexity leads to various signal integrity issues that arise due to parasitic components of the crossbar. A crossbar array architecture is designed using the extracted crossbar's parasitic components obtained using the Q3D extractor. The modeled architecture provides insight into the crossbar array's parasitic affect behavior at the schematic level for different real-time applications and how the parasitics of the crossbar will affect the fidelity and performance of the system. The proposed architecture uses a threshold-based post-synaptic neuron, which does not require any capacitor, unlike the LIF neuron, and occupies a smaller area. A neuron refractory controller is designed to make the training process efficient by keeping track of the neuron already fired and preventing it from firing in the consecutive training phase. The CMOS memristive synapse uses an average of $0.32\,nJ$ energy to recognize each pattern, much less than earlier works. The proposed architecture is validated using 180 nm CMOS technology.
12.	[Assessment of natural radioactivity in soil and water in the upper Himalayas region along the Manali–Leh highway, India](#) J Yadav, B Khyalia, N Kumar, A Panghal, PP Singh… - Journal of Radioanalytical and Nuclear Chemistry, 2023 **Abstract** This study represents the findings of the measurement of natural radioactivity in soil and water samples collected from the upper Himalayas region along the Manali–Leh Highway. The activity concentration values of terrestrial radionuclides in soil samples are measured using an n-type HPGe detector. The radiological hazards are also estimated through the evaluation of radium equivalent activity (R_{eq}), external and internal hazard index (H_{ex}, H_{in}), alpha index (I_{α}), gamma index (I_{γ}), air absorbed dose, and indoor and outdoor effective dose. The level of Uranium in surface and ground water samples collected from the region is determined using the LED Fluorimetry technique. Annual effective dose, radiological and chemical toxicity risk, and

	hazards quotient due to the presence of uranium in water samples are also calculated. The values of these parameters are compared with permissible limits.
13.	[Automated agriculture news collection, analysis, and recommendation](#) SD Joy, N Goel - Agriculture-Centric Computation: International Conference on Agriculture-Centric Computation, 2023 **Abstract** A country like India mainly depends on the sector of agriculture. Most people's economies are intensely engaged in the field of agriculture. So, developing the agriculture sector will be an excellent benefit for any country. Nowadays, People can immediately find any solution regarding agriculture through technology's modernization. We can get any news from online articles anytime without any movement. Agriculture news should also be available in online news articles so that people who are intensely engaged with the agriculture field and economy can quickly get their valuable news. People must go through many online news sites to gather all the agriculture-related news. We have proposed an NLP-based solution so people can get all agriculture-related news in one place combining multiple features. In this process, we have collected many articles from multiple online newspapers and classified the agriculture news articles. For the classification process, we have applied several classification models. We have also added a machine learning-based model to check the duplication between news articles. Although, there will be multiple categories of agriculture news so that people can directly follow the news as they want. People will also be recommended articles based on content and times. So, Getting information about agriculture will be more straightforward for the farmer, and they can know about new technologies to apply in their work. Finally, in this proposed work, people can get all the essential agriculture news from various sources in one central point, including many exciting features.
14.	[Broadband and high-performance photodetector fabricated using large area and transfer-free 2D–2D PTS2/MOS2 heterostructure](#) G Bassi, R Wadhwa, M Kumar - Advanced Optical Materials, 2023 **Abstract** 2D transitional metal dichalcogenide (TMDC) materials have shown great potential in the optoelectronics and electronics field owing to their unique and favorable properties. However, developing high-performance broadband photodetectors in bare TMDC material is impeded due to their limited absorption and poor charge-carrier separation. The recent advancement in van der Waals heterostructure fabrication has exhibited a new path to improve the device performance. In the present work, a facile approach is presented to fabricate a large area of PtS_2/MoS_2 heterostructure, which demonstrates a broad spectral detection range from 400 to 1200 nm with high responsivity (30.2 A W^{-1}) and detectivity (1.12×10^{13} Jones) even under near-infrared (NIR) 900 nm light illumination at moderate bias. Moreover, the PtS_2/MoS_2 photodetector exhibits a much enhanced responsivity (97 times) and detectivity (33 times) compared with bare MoS_2. A rise/fall time of 11 ms/10 ms for the PtS_2/MoS_2 device represents its fast response speed. The X-ray photoelectron spectroscopy measurements reveal the type-I band alignment between the PtS_2 and MoS_2, which are further utilized to understand the charge carrier dynamics between the PtS_2 and MoS_2 interface. This work presents a simple strategy to synthesize scalable, high-performance broadband photodetectors for future optoelectronics applications.
15.	[Closed-form expressions of shear correction factor for functionally graded beams](#) A Amandeep, AK Pathak, SS Padhee - Journal of Applied Mechanics, 2023 **Abstract** In this work, closed-form expressions of shear correction factor (SCF) have been derived for beams with functionally graded material (FGM), through variational asymptotic method (VAM). An energy equivalence approach has been adopted between VAM and Timoshenko model, for

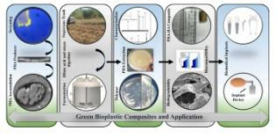|	
	estimating the SCF. A planar FGM beam has been considered and the calculation for SCF has been carried out. The formulation has been derived in a functional form that permits solutions for a large class of gradation models of FGM. In the limiting case when the material becomes homogeneous the estimated SCF matches exactly with that of the literature, thus validating the solution. A detailed discussion has been carried out on the results and conclusions have been drawn.
16.	Conceptual design of wireless smart grid for the optimization of electric transmission in Iraq AB Abbas, AA Almohammedi, … S Darshi - 3rd International Conference on Computing and Information Technology (ICCIT), 2023 **Abstract** Rapid development of technology has resulted in a considerable increase in electricity consumption, which has created a barrier not only because of the generation but also in delivery. Thus, when demand increases, the complexity of the electrical network increases as a result of the increased need for improved dependability, efficiency, protection, energy, and environmental sustainability. According to the world bank statistics, Iraq's loss was 51% during distribution, and it is considered significantly high. This study proposes a wireless network-based design for detecting and optimizing Iraq's electricity distribution infrastructure. Moreover, the suggested module is composed of several data gathering methods that are required for the various paths of the power distribution systems. This design offers viable support for a variety of issues confronting Iraq's power distribution systems, including variable voltage levels caused by fluctuating electrical usage, power burglary, manual invoicing, and transmission line breakdowns. The suggested design is intended for use with single-phase power transmission systems; however, it may be adapted for use with three-phase power distribution systems with slight improvements. The introduction of this method will result in significant energy savings, allowing for the availability of electricity to a greater number of users than previously possible in a crowded place. The suggested smart grid design, which was created for the Iraq context, permits real-time control of energy consumption, optimal electricity consumption, minimal loss, diagnosis of power failures, breakdowns, and automatic invoicing.
17.	Development of robotics in vegetable seedling transplantation: a future research direction A Sharma, L Kumawat, A Singh, International Journal of Vegetable Science, 2023 **Abstract** Robotics is playing a role in changing the face of agriculture. The combination of robot competencies, vegetable seedling culture, and operational settings is required when using robotics in vegetable transplanting. A manipulator mechanism and control are used for path determination, picking, and placing of the seedling using an end-effector. Seedlings are fragile, and while handling seedlings through a robotic system, physical strength and morphology must be considered to design the end effector. This article explores multiple aspects and instances of robotics development for vegetable seedling transplanting following a review of the fundamental components of plant production robots. The recent work with robots on vegetable transplanting techniques is addressed. Even though robots are becoming inseparable aspects of modern farming.
18.	Diagnosis of Alzheimer's disease via Intuitionistic fuzzy least squares twin SVM MA Ganaie, A Kumari, A Girard… - Applied Soft Computing, 2023 **Abstract** Neurodegenerative disorders like Alzheimer's disease (AD) are irreversible and show atrophies in the area of the cerebral cortex of brain. AD leads to loss of memory and other cognitive impairments. The AD subjects are evaluated based on magnetic resonance imaging scans. The data may have the problem of class imbalance, noise and outliers which is a great challenge for

	classification. Support vector machines and twin support vector machine-based classifiers may not effectively deal with these problems as both these models assume that all the samples are equally important for the separating hyperplane. To overcome these issues, we propose intuitionistic fuzzy least square twin support vector machine for class imbalance problems (IFLSTSVM) and class specific-IFLSTSVM (CS-IFLSTSVM). To minimize the effects of class imbalance, the samples are appropriately weighted to minimize their effect on the optimal hyperplane. Moreover, we use intuitionistic fuzzy scores to overcome the issues of noise and outliers. Intuitionistic fuzzy score values generate appropriate weights by considering both the distance of the samples from the class centroid as well as the heterogeneity of the samples. The proposed models IFLSTSVM and CS-IFLSTSVM are efficient as they need to solve a system of linear equations. In Alzheimer's disease diagnosis, the proposed IFLSTSVM and CS-IFLSTSVM models showed better performance in MCI_vs_AD and CN_vs_MCI cases, respectively. Moreover, the proposed models showed better performance in the diagnosis of breast cancer classification. The statistical analysis carried out over KEEL and UCI data leads to the superiority of the proposed models. The source code of the proposed model is available at https://github.com/mtanveer1/Diagnosis-of-Alzheimer-s-disease-via-Intuitionistic-fuzzy-least-squares-twin-SVM
19.	Discontinuities of free theories on AdS $_2$ JR David, E Gava, RK Gupta… - Journal of High Energy Physics, 2023 **Abstract** The partition functions of free bosons as well as fermions on AdS $_2$ are not smooth as a function of their masses. For free bosons, the partition function on AdS $_2$ is not smooth when the mass saturates the Breitenlohner-Freedman bound. We show that the expectation value of the scalar bilinear on AdS $_2$ exhibits a kink at the BF bound and the change in slope of the expectation value with respect to the mass is proportional to the inverse radius of AdS $_2$. For free fermions, when the mass vanishes the partition function exhibits a kink. We show that expectation value of the fermion bilinear is discontinuous and the jump in the expectation value is proportional to the inverse radius of AdS $_2$. We then show the supersymmetric actions of the chiral multiplet on AdS $_2 \times$ S ^{1} and the hypermultiplet on AdS $_2 \times$ S ^{2} demonstrate these features. The supersymmetric backgrounds are such that as the ratio of the radius of AdS $_2$ to S ^{1} or S ^{2} is dialled, the partition functions as well as expectation of bilinears are not smooth for each Kaluza-Klein mode on S ^{1} or S ^{2}. Our observation is relevant for evaluating one-loop partition function in the near horizon geometry of extremal black holes.
20.	Dual-branch convolutional neural network for robust camera model identification[Formula presented] K Rana, , P Goyal, G Sharma - Expert Systems with Applications, 2024 **Abstract** Identifying the model of the camera used for image capture is very useful in image forensics. To exploit complementary camera model specific features, we propose a dual-branch convolutional neural network (CNN) for camera model identification (CMI), where one branch directly uses the three-channel RGB image and the other uses a noise image obtained via high-pass filtering. For scalability, the approach operates on cropped image patches and majority voting is used for image-level CMI. We conducted extensive experiments to evaluate the proposed method on multiple datasets and compare its performance against prior approaches. For quantifying CMI accuracy, we use existing patch and image level (accuracy) metrics and also a new metric that we propose for assessing the robustness of image-level camera model estimates. Importantly, our evaluations and performance comparisons include: (a) datasets that are more representative of real-world application scenarios of current interest, where the images have undergone unknown processing as a result of sharing on social media platforms, and (b) cross-dataset scenarios where the evaluation is performed on a dataset different from and not necessarily represented by the

	training dataset. Our results demonstrate that the proposed approach offers improvements over the prior techniques, with particularly significant gains in accuracy for the social media dataset and for cross-dataset robustness assessment. The significant improvements over prior approaches that have used a single RGB or noise branch support our hypothesis that the proposed dual-branch architecture provides a convenient mechanism to introduce a favorable inductive bias in CNN architectures for CMI. © 2023 Elsevier Ltd
21.	[Ecological worldview moderates the mediation of implementation-intentions found in the relationship between ecological concerns and pro-environmental behaviour](#) N Mishra, A Mishra, P Singh - Asian Journal of Social Psychology, 2023 **Abstract** Even after adopting various measures, recent years have witnessed a surge in environment-related issues such as pollution and climate change. These issues have been considered anthropogenic, and it is a well-received notion that changing human behaviour is crucial for sustainable development. Promoting pro-environmental behaviour (PEB) requires understanding of associations among relevant factors; the present study aimed to explore the same among a few less-explored constructs, which, along with other factors, may significantly explain pro-environmental behaviour. The study examined the direct relationship of PEB with ecological intelligence (EI) and self-transcendent values. Also, it explored the mediating effects of implementation-intentions and the moderating effect of the "new ecological paradigm" (NEP) on PEB. The data were obtained from 400 adult participants using a set of standardized questionnaires. The results showed significant direct and indirect associations among EI, self-transcendent values, implementation-intentions, the NEP and PEB. Implementation-intentions significantly mediated the relationship of EI and values with PEB, and the mediation was moderated by the NEP. Individuals low on EI but endorsing the NEP showed implementation-intentions similar to those with high EI. Knowledge of the interplay among these factors can be utilized to design interventions for promoting PEB.
22.	[Effect of thermodynamic instability on viscous fingering of binary mixtures in a Hele-Shaw cell](#) MC Kim, L Palodhi … M Mishra - Journal of Fluid Mechanics, 2023 **Abstract** The coupled effects of thermodynamic and hydrodynamic instabilities are studied during viscous fingering (VF). We introduced a modified Cahn–Hilliard phase-field model in conjunction with the Korteweg force in the classical VF model and derived consistent governing equations. The free energy of the partially miscible system is described using a modified Flory–Huggins model, which allows us to investigate the temporal evolution of spatial inhomogeneities. The mass flux in the Cahn–Hilliard equations is modified according to modern diffusion theory. The governing equations have been solved through an in-house model implementation using the COMSOL multiphysics software. We successfully demonstrated the transition from the finger-like structures to the droplet formation during spinodal decomposition as demonstrated experimentally in the literature. Our results are also in agreement with earlier numerical results obtained using a classical Landau type mixing energy. We further systematically studied the effects of the Margules parameter (interaction parameter) and the gradient parameter, which is associated to the thermodynamic length scale and capillary number on the VF. Aysmmetric features of the binary mixture are also investigated showing a stronger thermodynamic effect on the system with increasing phase separation and, hence, droplet formation.

23.	[EmotiW 2023: Emotion Recognition in the Wild Challenge](#) A Dhall, M Singh, R Goecke… - ICMI '23: Proceedings of the 25th International Conference on Multimodal Interaction, 2023 **Abstract** This paper describes the 9th Emotion Recognition in the Wild (EmotiW) challenge, which is being run as a grand challenge at the 25th ACM International Conference on Multimodal Interaction 2023. EmotiW challenge focuses on affect related benchmarking tasks and comprises of two sub-challenges: a) User Engagement Prediction in the Wild, and b) Audio-Visual Group-based Emotion Recognition. The purpose of this challenge is to provide a common platform for researchers from diverse domains. The objective is to promote the development and assessment of methods, which can predict engagement levels and/or identify perceived emotional well-being of a group of individuals in real-world circumstances. We describe the datasets, the challenge protocols and the accompanying sub-challenge.
24.	[Endurance study of silicon-doped hafnium oxide (HSO) and zirconium-doped hafnium oxide (HZO)-based FeFET memory](#) P Duhan, T Ali, P Khedgakar… - IEEE Transactions on Electron Devices, 2023 **Abstract** We report a detailed characterization of the fluorite-structure-based Si:HfO2 (HSO) and Zr:HfO2 (HZO) ferroelectric (FE) materials integrated into a metal–FE–insulator–semiconductor (MFIS) FE field-effect transistors (FeFETs) gate-stack with the silicon oxynitride (SiON) interface layer. The pressing issue in the emerging FeFET concept is the limited endurance range (104–105) of program/erase cycles and is attributed to the gate-stack degradation. In a gate-first scheme, the effect of dopant type on the endurance performance of the fluorite structure-based FeFETs is investigated. The zirconium (Zr)-doped FeFETs show faster memory window (MW) degradation when compared with silicon (Si)-doped hafnium dioxide (HfO2) FeFETs. The physical mechanism responsible for endurance degradation is identified and attributed to the higher number of traps in the HZO-based FeFETs compared with the HSO ones.
25.	[Enhancement of plasmonic response by piezoelectrically deposited gold films](#) GP Singh, S Samanta, A Pegu, SS Yadav, U Singhal…N Sardana - Indian Journal of Physics, 2023 **Abstract** Thin film continuity using different fabrication processes is crucial in deciding its plasmonic response. The surface plasmon (SPR) response of gold films of various thicknesses deposited with and without a quartz base oscillating at 6 MHz was studied. The presence of the oscillating piezoelectric base resulted in a decrease in the surface roughness of the gold film. The 40 nm thick film displayed the best SPR response among the various thicknesses tested. The 40 nm film deposited piezoelectrically had a Q factor increase and an increased slope of the angle and wavelength dependent resonance curve as compared to 40 nm thick film not deposited piezoelectrically.
26.	[Engineering the porosity and active sites in metal-organic framework](#) AK Kar, GS More, R Srivastava - Catalysis in Confined Frameworks: Synthesis, Characterization, and Applications: Book Chapter, 2023 **Abstract** The endless structural features make the metal–organic framework (MOF) one of the promising classes of modern-day material. The basic features associated with MOF structure are high surface area, unique structural properties, and tunable chemical functionality. MOF is a highly crystalline material with a large surface area and a diverse range of tailorable porous framework structures. The porous framework structure of MOF arises due to the self-assembly of organic linkers (ligands) and metal nodes. Therefore,

	the possible active sites in MOF are located near the pores, metal nodes, and ligand centers. The functional tunable properties of MOF provide numerous opportunities for structural modifications and make them ideal for highly efficient catalytically active material by active site engineering of pores, metal nodes, and ligand centers. The resultant structurally modified MOFs are a unique class of catalytic material and have been successfully employed in several heterogeneous catalytic transformations. Additionally, MOF tends to carry homogeneously distributed metallic sites or other nanoscopic guest particle as the additional active centers, which can be used for a selected appointed catalytic reaction. The major challenges associated with the structurally modified MOF through active site engineering are their controlled synthesis strategies, the exact estimation of the modifications, and the apparent stability of the modified MOF. The idea of MOF framework modification is attributed to the modifications in the physical and chemical environment of the framework regions where the framework stability and reactivity altered and ultimately brought different interactions with the target species for organic transformation.
27.	[Estimation of lacunar permeability in anatomical regions of femoral cortex: endocortical versus periosteal](#) S Tiwari, R Kumar, … N Kumar… - Lecture Notes in Mechanical Engineering, 2023 **Abstract** Bone's adaptation occurs in response to mechanical loads. In vivo experimental studies explained that cortical bone envelopes (periosteal and endocortical) and their anatomical regions (anterior, posterior, lateral, medial) experience differential loading-induced osteogenesis. It has always been a challenge to establish a computer model to precisely predict such non-uniform new bone formation at the cortex due to mechanobiological stimuli such as strain or canalicular fluid flow. Lacunar permeability governs canalicular fluid velocity magnitude in bone-cross section. Anatomical variations of permeability could be the reason of differential fluid flow response which causes distinct site-specific bone formation. Therefore, it is important to compute poromechanical properties which are required to compute flow distribution. Lacunar canalicular permeability of the periosteal and endosteal surfaces in different anatomical locations has not been well reported. Thus, this paper estimates the poromechanical properties of cortical bone specially the permeability at periosteal and endocortical envelopes in their different anatomical regions, i.e. medial, lateral, anterior and posterior. Nanoindentation technique in combination with poroelastic optimization technique was employed. The result indicates that the endocortical surface was found to be more permeable than periosteal surface. Moreover, medial and lateral sides were also found more permeable than the other two regions, namely anterior and posterior. A clear understanding on cortical bone permeability will help researchers to precisely simulate the site-specific osteogenesis.
28.	[Exploring a-site cation variations in Dion–Jacobson two-dimensional Halide Perovskites for enhanced solar cell applications: a density functional theory study](#) HL Kagdada, B Roondhe, V Roondhe, SD Dabhi…R Ahuja - Advanced Energy and Sustainability Research, 2023 **Abtsract** The exceptional photophysical and electronic properties of 2D hybrid perovskites possess potential applications in the field of solar energy harvesting. The present work focuses on the two systems, exhibiting the Dion–Jacobson phase of 2D perovskite consisting of methylammonium (MA) and formamidinium (FA) cations at A-site and 3-(aminomethyl)pyridinium (3AMPY) as ring-shaped organic spacer. Altering A-site cations creates a distortion of inorganic layers and hydrogen bond interactions. It has been noted that the angles of Pb–I–Pb and I–Pb–I are more symmetric (close to 180°) for $(3AMPY)(MA)Pb_2I_7$ compared to $(3AMPY)(FA)Pb_2I_7$ and result in increase of bandgap from 1.51 to 1.58 eV. This further leads to a significant difference in Rashba splitting energy under the influence of spin-orbit coupling effects, where the highest splitting (36 meV) is calculated for conduction band edge of the $(3AMPY)(FA)Pb_2I_7$, suggesting the promising applications toward

	spintronics. The calculated absorption spectra cover the range from 300 to 450 nm, indicating significant optical activity of 2D $(3AMPY)(MA)Pb_2I_7$ and $(3AMPY)(FA)Pb_2I_7$ in the visible and ultraviolet regions, which bodes well for their application in advanced optoelectronic devices. The bandgap and high absorption coefficients present more than 30% of theoretical power conversion efficiency for both systems, as calculated from the spectroscopic-limited maximum efficiency.
29.	Exploring neurophysiological responses to cross-cultural deepfake videos MR Khan, S Naeem, …. A Dhall… - ICMI '23 Companion: Companion Publication of the 25th International Conference on Multimodal Interaction, 2023 **Abstract** Deepfake videos, which use artificial intelligence techniques to create realistic but fabricated footage, have raised concerns regarding their potential to deceive and manipulate viewers. This study is one of the first of its kind that aimed to investigate the cross-cultural perception of deepfakes and uncover potential neural markers associated with their detection. Electroencephalography (EEG) data were recorded from 10 healthy participants while they viewed three categories of videos: Asian people speaking Chinese (C-C), Asian people speaking English (C-E), and Middle Eastern people speaking English (A-E). Participants were asked to determine whether each video was real or fake. Behavioral analysis revealed that participants performed better in differentiating real and deepfake videos when the provided visual stimulus was in a language they were familiar with (English) and when the actor belonged to an ethnically similar background. EEG analysis demonstrated significant differences in brain signals between the three categories, suggesting the potential use of EEG as a biomarker for deepfake classification. Machine learning models achieved accuracies of up to 84.52% in categorizing the EEG data while observing real vs. fake videos, with Support Vector Machines. These findings contribute to our understanding of deepfake perception, have implications for the development of deepfake detection methods, and highlight the importance of media literacy in the face of digital deception.
30.	Extrapolation with range determination of 2-D spectral transposed convolutional neural network for advanced packaging problems Y Guo, X Jia… R Sharma - IEEE Transactions on Components, Packaging and Manufacturing Technology, 2023 **Abstract** In this article, we propose the application of a 2-D spectral transposed convolutional neural network (S-TCNN) with extrapolation to reduce the number of trainable parameters during the upsampling process, leading to reduced training time and a decrease in computational resources. Our proposed model consists of three stages, namely the prediction stage that uses high-accuracy 2-D S-TCNN to predict partial frequency responses; the extrapolation stage that takes the output of the prediction stage and uses the Gaussian process (GP) to construct the mean and covariance matrix; and the extrapolation range determining stage responses to numerically compute the optimized output length. For extrapolation, we construct new kernel combinations and use maximum likelihood estimation (MLE) to address the problem of losing correlation between priors and extrapolated points as distances increase. We also form a quantitative method to determine the extrapolation range, which takes the distance and confidence interval (CI) into consideration. We apply our method to three application examples: 1) a staggered via; 2) an on-chip microstrip line; and 3) an 1×8 slot antenna array. Results show that our model can reduce about 20% of the trainable parameters, 30% of memory storage, and 20% of the training time compared with the 2-D S-TCNN. The proposed method can also achieve a similar normalized mean-squared error (NMSE) level with a small tradeoff in the final loss.
31.	Fabrication of HA Nano-crystal Reinforced PHAs based composites for orthopedic fracture-fixing accessories using sustainable resources

P Tomer, GK Shroti… N Kumar - Environment, Development and Sustainability, 2023

Abstract
The increasing demand for biodegradable polymers in orthopedic applications has significant potential to be used as temporary implants. In this regard, metallic implants are already being used in biomedical fields for permanent implants. These implants are non-biodegradable, and re-surgery is required for their removal after healing. Polyhydroxybutyrate (PHB) becomes the major focus of attention in biomedical implants because it is temporary and is resorbed by the tissues after healing. In the present study, bacterial isolate Bacillus endophyticus BE01HL001 was used to produce PHB using pentosan-rich sugarcane trash hydrolysate and evaluate their functional and biological properties. The chemical and structural composition of extracted PHB has also been determined. The extracted PHB shows high thermal stability at 267 °C using differential thermal analysis (DTA). The major limitation of PHB is its low osteoconductivity, which restricts its use in orthopedic applications. Therefore, an attempt has been taken to improve the bioactivity of PHB by reinforcing it with bioactive ceramic hydroxyapatite (HA). The degree of crystallinity of PHB/HA composites increases from 71 to 89% with an increase in HA (5% to 20%). Due to the agglomeration, the decrement in tensile strength was observed with an increment of nano-sized HA, and in vitro evaluation in simulated body fluid (SBF) for up to 28 days showed enhanced apatite layer formation and significant degradation resistance of the composite structure. In vitro cytotoxicity assay revealed high growth and proliferation of osteosarcoma cells on HA-reinforced PHB composite. These attributes of PHB/HA composites make it suitable for use in orthopedic fracture-fixing accessories.Please check the edit made in the article title.We have checked the edit made in the article title and approved the same.

Frequency analysis incorporating a decision support system over Mahanadi catchment in India
N Gupta, SR Chavan - HYDRO 2021: Flood Forecasting and Hydraulic Structures: International Conference on Hydraulics, Water Resources and Coastal Engineering, 2023

Abstract
Different statistical criteria used for selecting the best fit for distributions are usually "biased" against the tail (large extreme events) as they give more weightage to the central tendency of the distribution. The extreme events are generally designated as the improbable events or outliers having less frequency of occurrence, resulting in the erroneous estimation of their magnitude and frequency. The present study evaluates the usefulness of the decision support system (DSS) to find a suitable class of probability distribution functions depending upon the tail heaviness. DSS analyzes the tail behavior of the sample data based on various graphical methods, viz., mean excess function plot, hill plot, log–log plot, max-sum ratio plot, and concentration profile. Once the distribution class is identified, the best fit distribution from various distributions in the class can be explored. The utility of the DSS is demonstrated through an application to the extreme precipitation data over the Mahanadi River basin. We have considered the gridded precipitation data obtained from the Indian Meteorological Department (IMD)-Pune having a resolution of 0.25°. Results show that almost all the graphical techniques combined to form a decision support system allow us to discriminate the exponential tail with a heavy tail, and one should rely on more than one graphical method for rational conclusions.

Full CMOS analog circuit implementation of multi-functional pavlov associative memory using STDP learning
SK Vohra, M Sakare, DM Das - IEEE Women in Technology Conference (WINTECHCON) ,

2023

Abstract
This paper demonstrates the complete Pavlov associative memory at the CMOS transistor level. Unlike many works focusing on digital implementation with area-intensive and power-hungry circuits, the proposed design for Pavlov associative memory is realised in the analog domain. Apart from learning and forgetting shown in various literature, the proposed circuit for Pavlov associative memory also incorporates the other biologically inspired functions of associative memory, such as learning with stimuli interval, variable learning rates, and generalisation and differentiation. Besides, most papers employ Pavlov training by forming a strong synaptic connection between the sensory auditory and output salivary neurons. In contrast, the actual Pavlov conditioning strengthens the synaptic connection between the auditory and gustatory neurons, as implemented in this paper. Unlike many works that use software-based SPICE models of a memristor as a synapse, the complete system uses on-chip trainable CMOS STDP memristive synapses and LIF neurons. The post-layout simulations of the proposed circuit implemented in TSMC 180 nm CMOS technology verify the functionality of the complete system.

34.

GraphITTI: attributed graph-based dominance ranking in social interaction videos
S Sharma, S Ghosh, A Dhall… - ICMI '23 Companion: Companion Publication of the 25th International Conference on Multimodal Interaction, 2023

Abstract
Estimating the most dominant person in a social interaction setting is a challenging feat even with the advancement of deep learning techniques due to problem complexity, non-availability of labelled data and subjective biases in annotations. This paper aims to reformulate the problem of detecting the Most Dominant Person (MDP) as a person ranking problem by utilizing person-specific attributes such as facial gestures, eye gaze, visual attention and speaking patterns. Our proposed framework, attributed Graph-based dominant person ranking in social InTeracTIon videos, GraphITTI, learns generic and robust person rankings on top of context level features. To inject domain knowledge into the GraphITTI framework, we consider inter-personal and intra-personal aspects along with spatiotemporal context patterns. Our extensive quantitative analysis suggests that GraphITTI framework performs favourably over the current state-of-the-art for dominant person detection and ranking.

35.

Green hydrogen production from biomass - A thermodynamic assessment of the potential of conventional and advanced bio-oil steam reforming processes
PP Singh, A Jaswal, R Singh, T Mondal… - International Journal of Hydrogen Energy, 2023

Abstract
Steam reforming of bio-oil derived from biomass pyrolysis is one of the most promising methods for the production of green hydrogen with minimal carbon footprint. In this context, this work investigates the thermodynamic potential of hydrogen production from bio-oil steam reforming. Four routes – conventional steam reforming (CSR) and three advanced reforming processes – sorption-enhanced steam reforming (SESR), chemical looping steam reforming (CLSR) and sorption-enhanced chemical looping steam reforming (SE-CLSR) - were modeled for this purpose. Bio-oil was modeled as a complex mixture of model compounds belonging to all major oxygenate families in order to have a closer resemblance with raw bio-oil. CaO was selected as the sorbent, while NiO was selected as oxygen carrier. Furthermore, the effect of process parameters such as steam to carbon, sorbent to carbon, oxygen carrier to carbon ratios, and reforming temperature was explored. H_2 purity and yield along with energy demand, served as the parameters for comparing the performance of the four processes. SESR provided the highest H_2 yield (0.216 kg_{H2} $kg_{Bio\text{-}oil}^{-1}$) among all the processes under optimum conditions along with a purity greater than $99\,\%$. CLSR, meanwhile, had the lowest H_2 yield and purity (0.178

kg$_{H2}$ kg$_{Bio-oil}^{-1}$ and 64.6 %, respectively). The combined SE-CLSR process had H$_2$ yield greater than both CSR and CLSR (0.197 kg$_{H2}$ kg$_{Bio-oil}^{-1}$) and a H$_2$ purity greater than 99 %. High in-situ heat generation was noted in the reforming reactor for both SESR and SE-CLSR, pointing towards a good potential for auto-thermal operation. Overall, SE-CLSR process is a highly intensified process with substantially lower energy requirements than all the other processes. The results highlight that by combining CO$_2$-sorption and chemical looping with traditional reforming, H$_2$ can be obtained in higher yields and purity and lower energy consumption.

| 36. | High gain and efficiency triple u-shaped slots microstrip patch antenna for 5g applications |
| | AA Almphammedi, A Raad, S Darshi… - 3rd International Conference on Computing and Information Technology (ICCIT), 2023 |

Abstract
The 28 GHz band is a frequency band that has been allocated for use in 5G mobile communication networks. It is part of the millimeter wave spectrum, which is a range of frequencies between 30 GHz and 300 GHz. This study proposes and investigates the 28 GHz 5G networks. A modified single element patch antenna with three grooved U-shaped holes is shown and is used to indicate a high gain and Efficiency for 28 GHz 5G antenna. The proposed antenna consists of the radiation element on a RTRogers 5880 laminate and is actuated by a microstrip feedline. The proposed work includes the most desirable characteristics, such as small size, light weight, low-cost fabrication and wide operation up to 1.4 GHz (27.1 - 28.5 GHz). The proposed antenna design also offers a high efficiency up to 89.73 %, high gain up to 8.14 dBi, and return loss up to −30 dB, resulting in attractive performance. The results obtained show that the antenna is a viable candidate for 5G applications at 28 GHz.

| 37. | Information processing from electronic word of mouth: an integrative framework |
| | A Ahmed, Amritesh - International Journal of Electronic Marketing and Retailing, 2023 |

Abstract
The authors propose a model of electronic word-of-mouth (eWOM) processing that integrates the conflict monitoring and the self-validation hypotheses. The model brings novel insights into the processing of eWOM by stressing cognitive conflict, a defining characteristic of eWOM. Extant models build on the notion that persuasion is inherent in eWOM and fail to account for what causes elaboration. This paper conceptualises eWOM-section as a gestalt of cues varying in their demand for cognitive resources, and the proposed model accounts for attitude appraisals relative to initial attitude. Also, eWOM literature has largely ignored time, an essential factor in consumer decision making, implicit in the proposed model. The model is contrasted with an earlier integrative model, research propositions are drawn, and conceptual contributions and practical implications are discussed.

| 38. | Intelligent state estimation for fault tolerant integrated frequent RTO and adaptive nonlinear MPC |
| | G Bagla…J Valluru - Journal of Process Control, 2023 |

Abstract
Combinations of real-time optimization (RTO) and model predictive control (MPC) have been widely employed in the process industry for tracking the economic optimum in the face of drifting disturbances and parameters. Online update of model parameters is a critical step in the implementation of RTO. In this work, an intelligent state and parameter estimation approach is developed by combining a fault diagnosis approach with a simultaneous state and parameter estimator. Since faults are more likely to develop as slow drifts, a nonlinear generalized likelihood ratio (GLR) approach available in the literature is modified by considering ramp models for the progression of faults with time. When a fault is isolated by the fault diagnosis and identification (FDI) component, the magnitude of the isolated fault is refined using a moving window state and parameter estimator until the fault magnitude continues to change. The
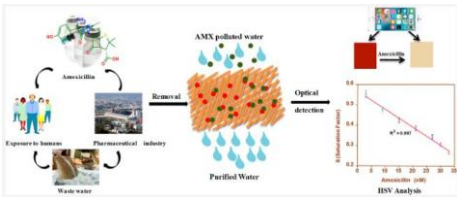
estimation of fault magnitudes is carried out only when required and triggered by the fault identification scheme. Thus, the subset of parameters/faults that are being estimated online can change with time. The intelligent state and parameter estimator is further combined with an online optimizing control scheme consisting of integrated frequent RTO and adaptive MPC. The integrated optimizing control scheme has embedded intelligence to auto-correct models used for estimation, control, and optimization and decide whether the detected changes require the invocation of RTO. The proposed approach employs a single model to carry out four different tasks: process monitoring, state and parameter estimation, nonlinear predictive control, and real-time optimization. This eliminates difficulties that can arise due to model mismatch between different components of the online optimizing control scheme. The efficacy of the proposed scheme is investigated using the benchmark Williams Otto reactor and a continuously operated fermenter. The economic optimum operating point of these systems is sensitive to mean shifts in unmeasured disturbances or system parameters. The proposed ramp model based approach successfully isolates the parameter/ unmeasured disturbance/ sensor bias/ actuator bias that has undergone slow drift and tracks the shifting economic optimum without significant delays. Thus, the proposed integrated approach has the ability to handle normal and abnormal operating envelopes of the system.

39.

Introduction to additive manufacturing: Concepts, challenges, and future scope
S Rathor, R Kant, E Singla - Industry 4.0: Concepts, Processes and Systems: Book Chapter, 2023

Abstract
Additive manufacturing (AM) includes a set of technologies to obtain a physical build part through the construction of all subsequent layers by adding material. Industry 4.0 aids the integration of production systems and innovative smart technologies. The Industrial Internet of Things (IIoT) can make production flexible, automated, and efficient. It allows machines to interact, exchange data, and process the same. The key benefits of AM in Industry 4.0 are decreased prototyping cost, time, digitization of the business, and assembly accumulation in a single part. The role of AM in Industry 4.0 is expounded through discussing different AM technologies and their working concepts with several potential challenging applications as per future requirements. This chapter will give the necessary concepts for understanding the digital technologies in AM.

40.

Investigation of mechanical and microstructural properties of sputter-deposited Zr-Ni_3Al coatings
SK Tiwari, AU Rao, AS Kharb, V Chawla, N Sardana… - Journal of Vacuum Science & Technology A, 2023

Abstract
Zr-doped Ni_3Al alloy coatings were deposited on a silicon substrate using DC magnetron cosputtering at a substrate temperature of $400\,°C$. The transformation of phase, microstructure, and surface topography was investigated using GIXRD, field emission scanning electron microscopy, and atomic force microscopy, respectively. The effect of zirconium (Zr) concentration on the microstructure and mechanical properties of Ni_3Al coatings has been discussed. It is observed that the high concentration of Zr in Ni_3Al coatings led to the evolution of microcracks that further contributes to increasing the surface roughness of the coatings. Results revealed that the Ni_3Al coating without Zr content exhibited the highest hardness of 12.8 GPa. It is also found that with the increase in Zr content in host Ni_3Al coatings, the hardness decreases, whereas the contact angle increases. Ni_3Al coatings with 40 W Zr enrichment showed a hydrophobic nature with a contact angle of $101°$.

41.

Investigations on the role of Inconel 82 additions on improving fatigue and corrosion behaviour of gas tungsten arc AISI 316L stainless steel claddings
H Kaur, D Malhotra… H Singh - Proceedings of the Institution of Mechanical Engineers, Part L:

Abstract
In the present work, single- and double-weld layers of Inconel 82 were added to 316L stainless steel claddings using the gas tungsten arc welding process with the aim of improving the fatigue and sensitization performance of such clad overlays. These overlays were subjected to a high-temperature sensitization treatment of 750°C/24 h (air-cooled) to induce precipitation, and then solution treated at 1050°C/2 h (furnace-cooled) to mitigate the ill effects of intermetallic precipitation. Carbides of types $Cr_{23}C_6$ and Cr_7C_3 were detected in the aged 316L clad, which occurred interdendritically. These deleterious phases decreased the fatigue crack growth resistance of conventional 316L, but the addition of Inconel 82 resulted in inducing crack-arresting tendencies in it and thus significantly increasing its resistance against fatigue crack propagation. Solution annealing treatment resulted in the dissolution of deleterious phases, due to which the fatigue performance of these clads improved significantly. Among all the specimens, 316L clad with the double layer of Inconel 82 in the solution-annealed condition offered the highest resistance to fatigue crack growth. Corrosion performance evaluated via sensitization studies shows that ageing degraded the corrosion performance of 316L weld overlays, but the addition of Inconel 82 improved it. This study establishes that the addition of Inconel 82 can significantly improve the fatigue and corrosion performance of conventional 316L weld claddings.

42.

Iodine functionalized 2,5-dimethoxy-2,5-dihydrofuran (DHFI) crosslinked whey protein-derived carbon nanodots (WCND) for antibacterial application
S Mukherjee, AK Pandey,… B Das… - Colloids and Surfaces B: Biointerfaces, 2023

Abstract
Whey protein-derived carbon nanodots (WCND) were synthesized using the microwave irradiation method, and its amine-rich surface functionality was crosslinked with covalently bound Iodine functionalized 2,5-dimethoxy-2,5-dihydrofuran (DHFI) to produce WCND-DHFI. The physicochemical characterization of both WCND and WCND-DHFI was performed and compared to comprehend the consequence of iodination on the characteristics of WCND. The suitability of CND in biological environments was evaluated through in vitro cytocompatibility and Chorioallantoic Membrane (CAM) assay, as well as a hemocompatibility study. WCND-DHFI has shown enhanced cell viability against WCND. Further, the antibacterial properties of both CNDs were studied against both gram-positive and gram-negative bacterial strains, representing an enhancement in antibacterial activity after DHFI crosslinking. WCND-DHFI has depicted a stable and prominent bacteriostatic activity for up to 6 h for both strains of bacteria. WCND-DHFI has denoted a 99.996% and 99.999% loss of bacterial viability for gram-positive and negative strains, respectively. Novel surface functionalization portrays an improvement in antibacterial activity. Transmission and scanning electron microscopy represent the cell wall rupturing by the WCND-DHFI, resulting in bacterial death. The ROS-mediated bacteriostatic mechanism of WCND-DHFI has been explored through assessing lipid peroxidation and protein oxidation assay. Moreover, the oxidative damage of DNA also has been explored. WCND-DHFI is performing as a promising cytocompatible and hemocompatible material for antibacterial applications.

43.

Jet or wet? Droplet post-impact regimes on concave contours
S Agrawal, G Khurana, D Samanta, P Dhar - The European Physical Journal E, 2023

Abstract
Droplet collision and subsequent spreading or wetting interactions with the solid substrate exhibit rich and interesting physics and are also important for various utilities. The fluid dynamics becomes more interesting and insightful when the wettability and geometry of the surface are tuned and altered. This study investigates the post-impact regimes of droplet impact on hydrophilic and superhydrophobic

	concave profile grooves (having dimensions comparable to that of the droplet). The post-collision hydrodynamics for such substrate-droplet system is three-dimensional, as in addition to droplet dynamics in the azimuthal direction, liquid jets may also be generated in the axial direction of the groove. Thereby the system may either lead to wetting or jetting, depending on the impact conditions. The effect of the impact Weber number (We) on the jet velocity, non-dimensional spreading width (γ) and non-dimensional south-pole film thickness (h^*) has been probed and quantified. The observations reveal that the role of the wettability of the substrate is more profound in the recoiling stage than in the spreading stage, because inertial forces dominate in the latter. It is also noted that the spreading width increases and south-pole height decreases with increasing the impact Weber number. The opposite trend is noted upon increasing the groove concavity by altering just one dimension of the groove. The jet velocity is found to be the highest immediately after the impact and eventually decreases in a nonlinear fashion. Further, it has been found that the jet velocity increases with increasing the impact Weber number and that this effect is more prominent for superhydrophobic surfaces. A semi-analytical framework has been proposed to predict the jet velocity evolution in terms of governing Weber (We) and capillary (Ca) numbers. The predictions of the proposed model are in good agreement with the experimental observations.
44.	Machine learning assisted manufacturing AK Gupta, A Kumar, NK Pande - Industry 4.0: Concepts, Processes and Systems: Book Chapter, 2023 **Abstract** Machine learning has found applications in all dimensions of human endeavours. In this chapter, we focus on machine learning-driven manufacturing. The chapter covers the important machine learning algorithms that help in automatising manufacturing which gives better quality assurance and higher production. The chapter aims to give a brief overview of two of the most sophisticated machine learning techniques, support vector machines and artificial neural networks. The chapter also deals with the prevalent problems in the manufacturing industry and their impact on the modern manufacturing process and environment and describes in detail how these problems can be tackled with the help of machine learning and artificial intelligence. Two of the most prevalent problems in the manufacturing industry are machinery malfunction and product quality control. The chapter aims to describe how we can implement the support vector machines and the artificial neural networks to predict these problems and keep the manufacturing process error-free, efficient, and able to manufacture products that are at par with the maintained quality standards.
45.	Mechanical and electromagnetic response of carbon fiber reinforced epoxy polymer composites at different orientations J Jyoti, GC Chauhan…A Kumar…M Sandhu…N Kumar - Polymer Composites, 2023 **Abstract** T-300 6K carbon fabric fiber-reinforced epoxy laminated composites are prepared by in-situ and hot-compression molding technique. The main emphasis of this study is to examine the impact of the structural deformations on fiber orientations of laminated composites during vibrational damping, stiffness, and electromagnetic interference (EMI) shielding properties. The damping properties of carbon fiber laminated composites are analyzed in terms of natural frequency and logarithmic decrement. The digital image correlation technique has been used to measure the mode shape behavior of carbon fiber reinforced polymer (CFRP) composites. The dynamic behavior of the CFRP laminated composites has significant effect on the fiber orientations in terms of storage, loss modulus, and damping ratio. The value of EMI shielding of CFRP laminated composites of T-300 6K based CFRP polymer laminated composites has slight variations in the SET and their values are 107.17 (B-45), 106.33 (B-30), and 110.0 dB (B-0). The vibrational and EMI shielding properties are showing a huge potential for these kinds of CFRP laminated composites in military and aircraft applications.
46.	Mechanical and morphological analysis of laser transmission welded dissimilar plastics using metal absorber

DK Goyal, R Kant - Optics & Laser Technology, 2023

Abstract
This study aims to investigate the laser transmission welding (LTW) of polystyrene and polycarbonate using an electrolytic iron powder absorber. For this purpose, the experiments are performed to explore the effect of laser power and scan speed on the weld strength and bond morphology. The lap shear tests are conducted to obtain the breaking force and ductility of the welded joints. The fractured surface and cross-sections are analyzed by scanning electron and optical microscopy to investigate the bond morphology and bonding mechanism of the weldments. The results show that laser power and scan speed significantly affect the weld strength and ductility of the joints. The optical and scanning electron micrographs clarify that mechanical anchoring of iron particles, polymeric interdiffusion, and small bubbles enhance the bond strength but thermal degradation, burning, and large bubbles negatively affect the bonding.

47.

Multi-temporal SAR Interferometry (MTInSAR)-based study of surface subsidence and its impact on Krishna Godavari (KG) basin in India: a support vector approach

A Tripathi, K Malik…RK Tiwari - Environmental Monitoring and Assessment, 2023

Abstract
The surface subsidence in the Krishna Godavari (KG) basin in India has increased with the discovery of crude oil and natural gas reserves since 1983. With private players coming up to bag the exploration and refining contracts, there must be timely monitoring of the surface subsidence of the region so that remedial measures for the resettlement of the populations can be taken promptly. Regular monitoring is necessary since the region is fertile and any seawater ingress results in the loss of valuable cultivable land. Multi-temporal SAR Interferometry (MTInSAR) technique has been applied successfully all over the world for the study and regular monitoring of land surface subsidence scenarios. This study utilizes data from Sentinel-1 C-band SAR sensor for MTInSAR-based surface subsidence and RADAR Vegetation Index (RVI)-based vegetation loss for the same season estimation between 2017 and 2022 for the KG basin region. It is inferred from the study that the region has shown surface subsidence of 80 mm/year between April 2020 and June 2022. This study uses support vector regressor (SVR) to predict the loss in forest cover in terms of RVI using MTInSAR-based surface subsidence, VH, and VV backscatter as parameters. It is observed that the SVR gave $R2$-statistics of 0.89 and 0.873 in the training and testing phases with a mean absolute error (MAE) and root mean squared error (RMSE) of 0.08 and 0.02, respectively. It is also observed that the region showed a loss of 3.21 km2 of cultivable land between 2020 and 2022.

48.

Novel single-stage and two-stage integrated magnetic chokes for dc-side emi filter in motor drive applications

S Singh, B Dwiza, K Jayaraman - IEEE Transactions on Power Electronics, 2023

Abstract
Passive electromagnetic interference (EMI) filters are widely used to suppress the conducted common-mode (CM) and differential-mode (DM) noise emissions. However, these passive EMI filters occupy a large PCB area and volume, reducing the power density of the converters. This paper proposes two novel integrated magnetic chokes for single- and two-stage EMI filters. Magnetic equivalent circuits for both the proposed integrated EMI chokes have been presented to estimate the inductance and magnetic flux density of the chokes. The flux distribution in the proposed integrated chokes for the DM and CM current excitation is validated through ANSYS simulation results. The performance of the proposed integrated chokes is experimentally presented and validated on a three-phase SiC inverter-fed Brushless DC (BLDC) motor drive. The proposed integrated choke for the single-stage EMI filter and the two-stage EMI filter reduces the PCB area by 37% and 36%, respectively, and the filter box volume is reduced by 34% and 9%, respectively when compared to their equivalent conventional EMI filters. The above-mentioned reduction has been achieved without significantly increasing the weight of the filter as compared to the weight of conventional EMI filters.

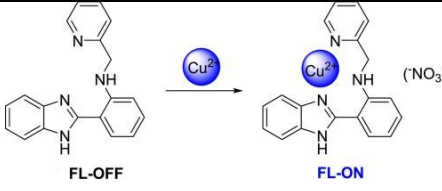|	
49.	[Numerical analysis of a helically corrugated tube using a novel combination of W/EG-based non-Newtonian hybrid nanofluid](#) A Painuly, NK Mishra, P Zainith, R Das - Numerical Heat Transfer, Part A: Applications, 2023 **Abstract** In this study, the second law analysis of a non-Newtonian hybrid TiO_2-SiO_2 nanofluid based on water/ethylene glycol has been carried out. The influence of the corrugation-height ratio (e/d_h) and volume fraction (φ) on the rates of entropy creation and exergy destruction are investigated using a helically corrugated tube. The model is simulated using ANSYS FLUENT 19.0 with the corrugated wall kept at a constant heat flux of $25\,kW/m^2$ and a range of hybrid nanofluid volume flow rates from 15 to 25 lpm. As the corrugation height and particle volume percentage increases, the HCT's rates of entropy generation and exergy destruction decrease. Additionally, as the volume flow rate of the hybrid nanofluid increases within the abovementioned range, the Bejan number and entropy generation number also decrease. For volume fraction of 5%, the Bejan number decreases to 0.873 at 25 lpm. The total irreversibility is reduced by adding corrugation and employing hybrid nanofluids. Also, working with the combination of corrugation and hybrid nanofluid leads to a notable increase in exergetic efficiency, reaching a maximum value of 82.8%.
50.	[Numerical investigation to enhance the thermal performance of solar air dryers using parallelogram type transverse ribs](#) MP Paulraj, SS Chandel, A Kumar, SK Sahu - Transactions of the Indian National Academy of Engineering, 2023 **Abstract** Present study reports the thermal performance of indirect type solar dryer (ITSD) with numerous roughness profiles through numerical investigation. The artificially roughened parallelogram transverse ribs (ARPTR) are integrated on the absorber plate of ITSD and numerical tests are carried out for various angle of attack ($\alpha = 30$–$150°$), relative roughness pitch ($P/e = 7.14$–14.28), relative roughness height ($e/D = 0.021$–0.042), and Reynolds number (Re $= 3800$–18000). The effect of α, P/e, e/D and Re on the thermo-hydraulic performance parameter (THPP), friction factor (f_r), and Nusselt number (Nu) are analyzed in the present study. The proposed ARPTR exhibits better performance compared to the proposed designs (circular and square roughened ribs) reported in the literature. The pressure drop is found to increase rapidly for the case of $P/e = 7$, i.e., the rib with larger height; while, the maximum value of pressure is found to decrease gradually with the increase in pitch roughness (P/e). The peak value of THPP is found to be 1.79 for $e\,P/e = 14.28$, $\alpha = 90°$, Re $= 3800$. The higher value of turbulent kinetic energy (TKE) is observed near the bottom of the absorber plate and it decreases in the downstream direction away from the absorber plate. The Peak TKE dissipation occurs between two ribs near the leading edge of the parallelogram ribs. The present design of ITSD with ARPTR exhibits 23.45, and 8.5% higher performance compared to square and circular roughened SAH reported in the literature.
51.	[Oxidation behavior of cocr$_{2-x}$feni$_{2.1}$nb$_x$ high entropy alloys](#) S Das, M Nagini, A Anupam…- Journal of Alloys and Compounds, 2023 **Abstract** High entropy alloys (HEAs) are one of the prominent alloy systems being studied for high-temperature applications. One of the key aspects to consider for high-temperature applications is to understand their oxidation behavior. When Nb is added as the alloying element to base FCC alloy like CoCrFeNi it promotes the formation of dual phase HEA. In the present study, the high-temperature oxidation behavior of annealed $CoCr_{2-x}FeNi_{2.1}Nb_x$ (x = 0.25, 0.5 and 1) isothermally at 800 °C in the air is studied. As-homogenized microstructure of these alloys shows a dual

phase containing FCC and Laves phase. The amount of Laves phase increases with increasing Nb content. The oxidation kinetics of the three compositions follows parabolic kinetics at 800 °C. The characterization (XRD, Raman, SEM) of the oxide layer reveals the formation of Cr_2O_3 as the main oxide layer. The cross-sectional SEM images of the oxide samples after 96 h of oxidation confirms absence of internal oxidation and a thin Laves-rich region below the Cr_2O_3 layer. The preferential formation of Cr_2O_3 over Nb oxides is explained using the assessment of their thermodynamic activity in the FCC phase.

52.

[Polyether sulfone-based organic nanoparticle coupled membrane for detection and purification of amoxicillin antibiotic from wastewater](#)
K Kaur, G Singh, N Kaur, N Singh - ACS EST Water, 2023

Abstract
Literature reveals that pharmaceuticals and derived metabolites are released continuously into the environment from point and nonpoint sources. Urban domestic effluents are the largest pathway of environmental pharmaceutical contamination and, thus, require improved treatment techniques to monitor and eliminate such contaminants from water and wastewater. In this regard, the present investigation describes the development of a self-assembled chemosensor using an azodye-based imine linked Co^{2+} complex (**R1.Co^{2+}**) that exhibits the potential for ratiometric and colorimetric quantification of AMX in buffer/aqueous media with a limit of detection = 0.717 μM and a limit of quantification = 4.14 μM. Further, the mechanism of detection of amoxicillin (AMX) has been explored through electrochemical studies, which reveals the oxidation of AMX by **R1.Co^{2+}** complex selectively, without any interference from other active analytes. The FE-SEM image reveals that the probe **R1.Co^{2+}** undergoes analyte-induced self-assembly, when interacting with AMX. Apparently, the **R1.Co^{2+}** complex was immobilized onto polyether sulfone (PES) membrane and evaluated for removal of AMX from environmental wastewater with adsorption capacity = 450.1 mg g^{-1} and removal efficiency = 90%. Moreover, the developed hybrid membrane can also be utilized as a solid-state colorimetric sensor of AMX, as revealed by the hue, saturation, and value (HSV) parameter model through a portable mobile-based prototype.

53.

[Quantum phases and the spectrum of collective modes in a spin-1 bose-einstein condensate with spin-orbital-angular-momentum coupling](#)
P Banger, A Roy, S Gautam - Physical Review A, 2023

Abstract
Motivated by recent experiments [Chen *et al.*, Phys. Rev. Lett. 121, 113204 (2018); Chen *et al.*, Phys. Rev. Lett. 121, 250401 (2018)], we investigate the low-lying excitation spectrum of the ground-state phases of spin-orbital-angular-momentum-coupled (SOAM-coupled) spin-1 condensates. At vanishing detuning, a ferromagnetic SOAM-coupled spin-1 Bose-Einstein condensate (BEC) can have two ground-state phases, namely, coreless and polar-core vortex states, whereas an antiferromagnetic BEC supports only polar-core vortex solution. The angular momentum per particle, longitudinal magnetization, and excitation frequencies display discontinuities across the phase boundary between the coreless vortex and polar-core vortex phases. The low-lying excitation spectrum evaluated by solving the Bogoliubov–de Gennes equations is marked by avoided crossings and hence the hybridization of the spin and density channels. The spectrum is further confirmed by the dynamical evolution of the ground

	state subjected to a perturbation suitable to excite a density or a spin mode and a variational analysis for the density-breathing mode.
54.	Rainbow in Gethen: Queer utopia and community collectivism in Ursula K. Le Guin's "Coming of Age in Karhide" AA Paul, KS Swathi - Literature Compass, 2023 **Abstract** This essay seeks to examine how Ursula K. Le Guin's science fiction short story "Coming of Age in Karhide" (1995) set in the planet of Gethen in the fictional Hainish universe envisions a political utopia of sequentially hermaphroditic humans to offer a succinct critique of traditional gender roles and conventional sexual customs while celebrating the potential of collective responsibility. While maintaining that the recent scholarship on queer utopias in SF has largely geared toward posthumanist articulations, the present essay argues that Ursula K. Le Guin who laid the genre conventions of queer utopic narratives unabashedly places her short story "Coming of Age in Karhide" within the ideals of humanism by upholding community as a unifying entity, at the same time carefully avoiding the pitfalls of anthropocentrism. Drawing from queer theorists and social scientists, this essay, while exemplifying the implications of a futuristic gender-neutral society, albeit partially, examines Le Guin's celebration of community collectivism in "Coming of Age in Karhide" to argue that the integration with the values and expectations of the larger community occasions individual growth and identity formation of the teenage protagonist and thereby, attests to the author's humanistic temperament.
55.	Real-time linear antenna array synthesis of broadside pattern using improved dwarf mongoose optimization algorithm H Singh, S Singh, A Gupta - Telecommunication Systems, 2023 **Abstract** This research introduces a novel framework that combines the dwarf mongoose optimization (DMO) algorithm with the sine–cosine algorithm (SCA) for the design of real-time linear antenna array (LAA) applications. The DMO algorithm, inspired by swarm behavior found in nature, comprises distinct groups—the alpha group, scouts, and babysitters—each utilizing unique food-capturing strategies. Linear antenna arrays are widely used in next-generation communication applications such as 5G, IoT and beamforming. However, it is challenging to achieve a narrow beamwidth while also suppressing subsidiary lobes. In this study, a novel approach is proposed to address this tradeoff successfully. Through thorough evaluations and comparisons with established strategies, the method demonstrates superior performance. It achieves the lowest subsidiary lobes and the narrowest beamwidth compared to other techniques. Moreover, the proposed framework consistently maintains optimal fitness values and offers highly efficient solutions, surpassing basic and popular optimization approaches. By optimizing excitation amplitudes and positions, the method successfully solves the narrow beamwidth limitation without sacrificing low side lobe levels (SLL). The research demonstrates that the proposed approach, combining DMO and SCA, effectively addresses the beamwidth-SLL tradeoff, making it capable of handling a wide range of LAA application requirements without compromising beamwidth or SLL. Overall, this study presents a significant advancement in LAA design, offering a novel variant of the DMO algorithm incorporating SCA, with improved performance and the potential for real-time linear antenna array applications.
56.	Real-Time prediction of in-hospital outcomes using a multilayer perceptron deployed in a web-based application V Nair, VP Nathasha, … AK Sahani - Lecture Notes in Networks and Systems, 2023 **Abstract** In-hospital mortality prediction in real time can offer clinicians a convenient and easy indicator of patient acuity and hospital efficiency. The latter also significantly relies on adequately

utilizing the hospital resources to deliver quality treatment and care. The provision of quality care merits the reduction of the average duration of patient stay, especially for intensive care units (ICU) where patients are in critical condition. Knowing the length of patient stay can thus serve as an indicator of hospital efficiency and help drastically improve hospital resource utilization. Also, extensive hospital stay usually denotes prolonged bed rest, the primary cause of pulmonary embolism (PE). We have also taken into cognizance that despite recent advancements in hospital infrastructures, cardiovascular disorders are a leading cause of mortality, among which heart failure (HF) and ST-elevation myocardial infarction (STEMI) have lately gained prominence. The advent of electronic health records (EHR) has allowed the usage of machine learning prediction algorithms to determine various health disorders from patient data. Therefore, we have developed sequential deep neural networks capable of predicting HF, STEMI, and PE from patients' demographic data, prior medical history, and initial lab parameters, with an AUC of 0.867, 0.861, and 0.761, respectively. We have also developed neural networks for predicting Mortality with an AUC of 0.985 and Duration of ICU and Hospital Stay with Mean Absolute Error of 2.03 and 2.54, respectively, by adding doctors' diagnoses of comorbidities to patient records. We have designed a web application that can be deployed in a hospital and used to test these models on real-time patient data.

57.	Reconfigurable robotic systems for Industry 4.0 E Singla - Industry 4.0: Concepts, Processes and Systems: Book Chapter, 2023 **Abstract** A robotic system happens to be an integral part of industrial automation and the diversity in such environments demand specialized designs of robotic manipulators and their work cells. With the rapidly growing range of less repetitive applications – the concept of customized robotic manipulators is emerging as the need of the day. Industry 4.0 involves timely data collection, timely status information, history, and target states, which help in optimal planning of production systems. Demand-based customized products can be planned for best utilization of resources and services. This involves highly flexible mass production that can be rapidly adapted to market changes. Work pieces, tools machines, and robots need to be capable of autonomously exchanging information, triggering actions, and controlling each other independently. New trends towards mass customization, small scale manufacturing, and maintenance services − which are non-repetitive in nature − require robotic manipulation systems with different configurations. Customized robot configurations are desired on a regular basis, to cope with the frequent changes in task and environment. To provide cost-effective solutions for rapid customization, modularity and re-configurability provide promising solutions. This chapter consists of the design of modular robotic systems, modular components, robot assembly, and reconfiguration possibility.
58.	Recycling of metal/polymer waste as a feedstock material via additive manufacturing technology: A review AD Patil, M Singh, S Chaudhary, H Singh - Industry 4.0: Concepts, Processes and Systems, 2023 **Abstract** Additive manufacturing (AM) has become one of the most revolutionary technologies in the manufacturing sector. AM technology is playing a vital role in Industry 4.0 because of its distinct advantages over conventional manufacturing, such as the ability to manufacture complex shapes with high efficiency, reduced lead time, waste minimization, fast prototyping, and in-house production. With the advancement in the field of AM technology, the size and cost of the printing machines are reduced; hence these techniques are becoming popular in various sectors like automobiles, aerospace, lab prototyping model, architectural models, printing electronics, and construction industry. Despite the recent research and developments in AM technology,

	there is still demand for improvements in feedstock materials and methods to match with the traditional manufacturing technologies for mass production. Manufacturing industrial waste, such as metal scrap and packing materials, is one of the biggest challenges for efficient production and environmental protection. Thus, the recycling of industrial waste as potential feedstock material for AM technology to produce useful products is highly desirable. This chapter provides an overview of the recycling and utilization of metallic and polymer waste as feedstock materials via AM technology.
59.	Reduction Kinetics of Composite Steel Slag-Coke Pellets C Ambade, SS Chandel & P K Singh - METCENT 2023: Proceedings of the International Conference on Metallurgical Engineering and Centenary Celebration, 2023 **Abstract** Generation of slag during steel making is a process consequence but it produces in high volume and management of such wastes is a primary environmental concern and a challenge also for the steel making industries. Steel slag is rich in mineralogy, such as iron oxides, calcium oxide, silicon oxide, magnesium oxide, manganese oxide, and aluminum oxide etc. Out of these, the major minerals in the steel slag are iron and calcium oxides. The iron content in such slag is 25–35%, which varies with steel production processes. Iron recovered from the slag can be used for secondary steel industry replacing a handsome amount of scrap. In this experiment, the kinetics has been investigated during the solid reduction of iron oxide from the slag are studied at different coke-to-slag ratios, different reduction temperatures for different reduction times. Here, the coke-to-slag ratio was taken as 0.5, 1, and 1.5 for reduction temperature 1000, 1100, and 1200 °C with 15, 45, and 120-min reduction time. The kinetic and reduction parameters like activation energy and pre-exponential factor for solid stage reduction of EAF slag are calculated with the help of Coats-Redfern methods.
60.	Response of the FAst TIMing array (FATIMA) for DESPEC at FAIR Phase-0 MMR Chisti, S Zazrawi… A Sharma… - Nuclear Instruments and Methods in Physics Research, Section A: Accelerators, Spectrometers, Detectors and Associated Equipment, 2023 **Abstract** The Monte-Carlo simulated response for γ-ray detection of the FAst TIMing Array (FATIMA) for exploitation within the DEcay SPECtroscopy (DESPEC) experimental system at the FAIR Phase-0 facility at Darmstadt, Germany is presented. In this configuration, FATIMA consisted of 36 $LaBr_3$(Ce) detectors surrounding the AIDA, position-sensitive charged-particle active stopper. The decay of the $I^{\pi}=8^+$ isomer-fed decay cascade in ^{96}Pd, measured in the first DESPEC experiment at the FAIR-0 facility was used to validate the simulations. The experimental data yielded in-situ full-energy peak efficiency values for FATIMA of 11.2(11)%, 6.8(7)%, 3.8(4)% and 2.1(4)% at 106, 325, 684 and 1415 keV respectively, consistent with the values derived from the simulated response
61.	Revolutionizing medicine with toll-like receptors: A path to strengthening cellular immunity JA Malik, G Kaur , JN Agrewala - International Journal of Biological Macromolecules, 2023 **Abstract** Toll-like receptors play a vital role in cell-mediated immunity, which is crucial for the immune system's defense against pathogens and maintenance of homeostasis. The interaction between toll-like-receptor response and cell-mediated immunity is complex and essential for effectively eliminating pathogens and maintaining immune surveillance. In addition to pathogen recognition, toll-like receptors serve as adjuvants in vaccines, as molecular sensors, and recognize specific patterns associated with pathogens and danger signals. Incorporating toll-like receptor ligands into vaccines can enhance the immune response to antigens, making them potent adjuvants. Furthermore, they bridge the innate and adaptive immune systems and improve antigen-presenting cells' capacity to process and present antigens to T cells. The

	intricate signaling pathways and cross-talk between toll-like-receptor and T cell receptor (TCR) signaling emphasize their pivotal role in orchestrating effective immune responses against pathogens, thus facilitating the development of innovative vaccine strategies. This article provides an overview of the current understanding of toll-like receptor response and explores their potential clinical applications. By unraveling the complex mechanisms of toll-like-receptor signaling, we can gain novel insights into immune responses and potentially develop innovative therapeutic approaches. Ongoing investigations into the toll-like-receptor response hold promise in the future in enhancing our ability to combat infections, design effective vaccines, and improve clinical outcomes.
62.	Seismic risk assessment of a Himalayan town: A case study of aueen of hills, Mussoorie, Uttarakhand, India K Modha, M Surana, … P Haldar… - Lecture Notes in Civil Engineering, 2023 **Abstract** The Himalayan region in north India is characterized by both mild-to-steep hill slopes as well as high seismicity. The presence of topographic features significantly alters the earthquake ground-motion characteristics in terms of both the amplitude and frequency content. In addition, the building configurations observed in these regions are also significantly different than those usually observed in the plain areas. As a result, hilly regions pose significantly higher seismic risk compared to their plain terrain counterparts with comparable seismicity. In the present study, probabilistic seismic risk assessment is conducted for a typical Himalayan town of Mussoorie, in the state of Uttarakhand, India. Firstly, the topographic amplification effects are estimated corresponding to various hill geometries using finite element simulations, and amplified seismic hazard maps are developed. The building stock inventory for the town is prepared using a combination of satellite imagery and random sample ground surveys. The available building fragility and vulnerability functions from the Global Earthquake Model along with the developed hazard and exposure models are integrated into OpenQuake to obtain seismic risk maps for Mussoorie, with and without considering the topographic amplification effects. It is shown that the topographic amplification effects alone can increase seismic losses up to ~200%, thereby highlighting a need to include them in seismic design of structures.
63.	Simple turn-on fluorescent chemosensor for ultrafast and highly selective trace-level detection of Cu^{2+} ions in aqueous solutions S Park, SY Bong, S Sharma, N Singh… - Spectrochimica Acta Part A: Molecular and Biomolecular Spectroscopy, 2023 **Abstract** A benzimidazole-based probe, BIPMA (2-(1*H*-benzo[*d*]imidazol-2-yl)-*N*-(pyridin-2-ylmethyl)aniline), was designed and synthesized to detect Cu^{2+} ions. BIPMA exhibited a fluorescent "turn-on" mechanism when bound to Cu^{2+} ions in an acetonitrile/water mixture (5:5, v/v, HEPES 10 mM, pH 7.4) owing to the synergistic effect of the chelation-enhanced fluorescence and internal charge-transfer mechanisms. Moreover, the BIPMA probe effectively detected nanomolar-range concentrations (0–400 nM) of Cu^{2+} ions in an aqueous system with a detection limit of 4.80 nM; this value is significantly lower than that set by the U.S. Environmental Protection Agency (≈20 µM). Additionally, BIPMA showed an ultrafast response to Cu^{2+} ions, with a maximum intensity achieved 25 s after adding Cu^{2+}. Furthermore, BIPMA detected Cu^{2+} ions in solutions with a pH range of 5–11, without being influenced by pH, underscoring its applicability under various physiological conditions. Density functional theory studies revealed that internal charge transfer was responsible for emission. Finally, BIPMA effectively detected Cu^{2+} ions in real water samples and living cells.

FL-OFF   Cu²⁺ → Cu²⁺   (⁻NO₃)   FL-ON

64.	[Smart sensors and actuators in Industry 4.0](#) H Gurung, R Kant - Industry 4.0: Concepts, Processes and Systems: Book Chapter, 2023 **Abstract** In the realm of automation and intelligent manufacturing, "Industry 4.0" plays an important role in the industry's extensive growth. Over the years, Industry 4.0 has evolved resulting in smarter manufacturing, thus providing an improved end product in terms of quality and productivity. Industry 4.0 brings more and more industrial axis of motion by introducing the Internet of Things (IoT) and information and communication technologies (ICT), where an interaction between the digital and real world occurs through smart sensors and actuators. Smart sensors collect information from the environment that further generates data corresponding to the information. In addition, smart sensors also perform self-monitoring and signal conditioning if required. Nowadays, smart actuators are also used widely in various industries. Smart actuators can do the self-monitoring and accordingly take a decision to provide a safety actuator operation. This chapter presents the applications of smart sensors and smart actuators in Industry 4.0.
65.	[Space-dependent intermittent feedback can control birhythmicity](#) D Biswas, T Mandal, PS Dutta… - Chaos: An Interdisciplinary Journal of Nonlinear Science, 2023 **Abstract** Birhythmicity is evident in many nonlinear systems, which include physical and biological systems. In some living systems, birhythmicity is necessary for response to the varying environment while unnecessary in some physical systems as it limits their efficiency. Therefore, its control is an important area of research. This paper proposes a space-dependent intermittent control scheme capable of controlling birhythmicity in various dynamical systems. We apply the proposed control scheme in five nonlinear systems from diverse branches of natural science and demonstrate that the scheme is efficient enough to control the birhythmic oscillations in all the systems. We derive the analytical condition for controlling birhythmicity by applying harmonic decomposition and energy balance methods in a birhythmic van der Pol oscillator. Further, the efficacy of the control scheme is investigated through numerical and bifurcation analyses in a wide parameter space. Since the proposed control scheme is general and efficient, it may be employed to control birhythmicity in several dynamical systems. Birhythmicity is a particular form of multistability. An unstable limit cycle acts as a separatrix between two limit cycles of the stable nature. It appears in several physical, engineering, and biochemical systems. It is undesirable in most systems, whereas in a few biological systems, it is helpful in biochemical organizations. Here, we propose a space-dependent intermittent control scheme to control birhythmicity for various dynamical systems ranging from physics and engineering to biology. The control scheme is based on space-dependent intermittent self-feedback. An exemplary birhythmic van der Pol oscillator is analyzed using harmonic decomposition and energy balance methods. The stability of the system is investigated using bifurcation analysis. We demonstrate the efficacy of the proposed control scheme in five real systems from diverse branches of natural science. We find that the scheme is efficient enough to control the birhythmic oscillations in all the systems.
66.	[Spatial concentration of Indian service industries in rural and urban areas: A micro-unit-level analysis](#) S Agrawal, SR Behera - Cogent Economics & Finance, 2023

Abstract
This paper explores the spatial concentration of 120 service industries in India's rural and urban areas, covering 33.60 million establishments using Economic census (2013) data at the district level. Besides, this study uses a cartogram map to examine knowledge-intensive business services (KIBS) industries' spatial concentration patterns and geographical concentration of employment of workers in rural and urban areas in India. Empirical results show that the magnitude of the spatial concentration effect varies in rural and urban areas. Further, empirical results reveal that KIBS industries are localized in rural and urban areas but have a skewed distribution toward urban areas. Moreover, results show that hotspots in rural areas seem higher than urban hotspots, although rural hotspots employ fewer employees than urban hotspots. The empirical results suggest that urban planners and district municipal authorities can give more emphasis and implement suitable KIBS industry-specific policies to boost regional economic growth and employment in rural and urban India.

67.

[Tailoring the Porosity and Active Sites in Silicoaluminophosphate Zeolites and Their Catalytic Applications](#)
JH Advani, A Kumar, R Srivastava - Catalysis in Confined Frameworks: Synthesis, Characterization, and Applications: Book Chapter, 2023

Abstract
Silicoaluminophosphate (SAPO) zeolites have emerged as attractive catalysts for various industrial applications due to their unique porosity and active sites. SAPOs are a family of crystalline microporous materials with customizable topologies and chemical compositions that make them appealing for various catalytic processes. This chapter provides insights into the porosity and active sites of SAPO zeolites and explores their catalytic applications in diverse chemical reactions, such as hydrocarbon conversion, selective oxidation, and acid-catalyzed processes. The fundamental characteristics of SAPOs and insights into the design and optimization of innovative SAPO-based catalysts with increased activity and selectivity would pave the path for developing new SAPO materials for their applications in petrochemical, fine chemicals, and renewable chemicals.

68.

[Ultralow lattice thermal conductivity and thermoelectric performance of twisted Graphene/Boron Nitride heterostructure through strain engineering](#)
N Gupta, S Rani, … R Ahuja, SJ Ray - Carbon, 2023

Abstract
We designed and investigated the electronic, mechanical, and thermoelectric properties of Graphene/hexagonal Boron Nitride (Gr/h-BN) heterostructure at various twisting angles based on the Ab-initio simulation. The structural stability was studied at optimized rotation angles (ϕ) = 0∘, 16.10∘, 21.79∘, 38.21∘, 43.90∘ and 60∘. The heterostructure shows semiconducting nature at ϕ=0∘, 21.79∘ and 38.21∘. These twisted heterostructures have demonstrated extraordinary mechanical properties such as Young's modulus and bulk modulus. Using the semiclassical Boltzmann transport theory, it is observed that the Seebeck coefficient, electric conductivity, and power factor at ϕ=0∘, 21.79∘, 38.21∘, and 60∘ are much higher than the values measured at ϕ=16.10∘ and 43.90∘. Moreover, at ϕ=60∘, the Power Factor for the n-type dopants can reach 1.37×10^{11} W/msK2. The lattice thermal conductivity at room temperature is found to be very low for ϕ=16.10∘, 21.79∘, 43.90∘ and 38.21∘ rotation angles. An ultralow lattice thermal conductivity with a value of 0.095 W/mK at 300K has been observed for 21.79∘ rotation angle, which is lower than other rotation angles because of very low group velocity (22.1 km/s) and short phonon lifetime (∼0.12 ps). The high thermoelectric performance results from an ultralow thermal conductivity arising due to the strong lattice anharmonicity. The present observations can offer significant impact on the design of high performance thermoelectric materials based on

	twisted van der Waals heterostructure (vdWH).
69.	[Vortex lattice formation in spin–orbit-coupled spin-2 Bose–Einstein condensate under rotation](#) P Banger - Journal of Low Temperature Physics, 2023 **Abstract** We investigate the vortex lattice configuration in a rotating spin orbit-coupled spin-2 Bose–Einstein condensate confined in a quasi-two-dimensional harmonic trap. By considering the interplay between rotation frequency, spin–orbit couplings, and interatomic interactions, we explore a variety of vortex lattice structures emerging as a ground state solution. Our study focuses on the combined effects of spin–orbit coupling and rotation, analyzed by using the variational method for the single-particle Hamiltonian. We observe that the interplay between rotation and Rashba spin–orbit coupling gives rise to different effective potentials for the bosons. Specifically, at higher rotation frequencies, isotropic spin–orbit coupling leads to an effective toroidal potential, while fully anisotropic spin–orbit coupling results in a symmetric double-well potential. To obtain these findings, we solve the five coupled Gross–Pitaevskii equations for the spin-2 BEC with spin–orbit coupling under rotation. Notably, we find that the antiferromagnetic, cyclic, and ferromagnetic phases exhibit similar behavior at higher rotation.